

2006

Nonlinear Model Predictive Control Technique for Unmanned Air Vehicles

Nathan Slegers

George Fox University, nslegers@georgefox.edu


Jason Kyle

Oregon State University

Mark Costello

Georgia Institute of Technology - Main Campus

Follow this and additional works at: https://digitalcommons.georgefox.edu/mece_fac

 Part of the [Aeronautical Vehicles Commons](#), [Military Vehicles Commons](#), and the [Navigation, Guidance, Control and Dynamics Commons](#)

Recommended Citation

Slegers, Nathan; Kyle, Jason; and Costello, Mark, "Nonlinear Model Predictive Control Technique for Unmanned Air Vehicles" (2006). *Faculty Publications - Biomedical, Mechanical, and Civil Engineering*. 5. https://digitalcommons.georgefox.edu/mece_fac/5

This Article is brought to you for free and open access by the Department of Biomedical, Mechanical, and Civil Engineering at Digital Commons @ George Fox University. It has been accepted for inclusion in Faculty Publications - Biomedical, Mechanical, and Civil Engineering by an authorized administrator of Digital Commons @ George Fox University. For more information, please contact arolfe@georgefox.edu.

Nonlinear Model Predictive Control Technique for Unmanned Air Vehicles

Nathan Slegers*

University of Alabama at Huntsville, Huntsville, Alabama 35899

Jason Kyle†

Oregon State University, Corvallis, Oregon 97331-4501

and

Mark Costello‡

Georgia Institute of Technology, Atlanta, Georgia 30332

A nonlinear model predictive control strategy is developed and subsequently specialized to autonomous aircraft that can be adequately modeled with a rigid 6-degrees-of-freedom representation. Whereas the general air vehicle dynamic equations are nonlinear and nonaffine in control, a closed-form solution for the optimal control input is enabled by expanding both the output and control in a truncated Taylor series. The closed-form solution for control is relatively simple to calculate and well suited to the real time embedded computing environment. An interesting feature of this control law is that the number of Taylor series expansion terms can be used to indirectly penalize control action. Also, ill conditioning in the optimal control gain equation limits practical selection of the number of Taylor series expansion terms. These claims are substantiated through simulation by application of the method to a parafoil and payload aircraft as well as a glider.

Nomenclature

b	= span
c	= chord
d	= control flap width
F_A	= aerodynamic force coefficient vector
F_c	= aerodynamic control force coefficient matrix
I	= inertia matrix of system with respect to its mass center
I_B, J_B, K_B	= body frame unit vectors
I_I, J_I, K_I	= inertial frame unit vectors
L, M, N	= aerodynamic moment components in the body reference frame
M_A	= aerodynamic moment coefficient vector
M_c	= aerodynamic control moment coefficient matrix
M_i	= relative degree for the i th output
p, q, r	= components of angular velocity of the system in body reference frame
Q	= diagonal tracking error weighting matrix
q_i	= tracking error weight on the i th diagonal of Q
R_i	= number of Taylor expansion terms in the i th output and desired trajectory approximation
S_i	= number of Taylor expansion terms in the i th control approximation
S_R	= reference area
\mathbf{u}	= control vector
u_b, v_b, w_b	= components of velocity vector of the system mass center in the body frame

V_A	= total aerodynamic velocity of the parafoil and payload system
X, Y, Z	= aerodynamic force components in the body reference frame
x_I, y_I, z_I	= components of position vector of the system mass center in an inertial frame
$\phi, \theta,$	= Euler roll, pitch, and yaw angles of system

I. Introduction

Unmanned air vehicles (UAVs) are providing improved capability in performing a diverse set of military missions such as reconnaissance, targeting, and civilian missions such as border patrol and environmental sensing. More aggressive use of UAVs promises to yield new capability such as adaptive battlefield communication networks, autonomous equipment delivery, flexible autonomous traffic monitoring, and massively parallel autonomous search and rescue. A key element in these systems is the autonomous flight control system. Many different control strategies have been developed specifically for highly nonlinear dynamic systems such as UAVs including feedback linearization, sliding-mode control, and fuzzy logic [1–3].

Model predictive control laws use a dynamic model of the plant to project the state into the future and subsequently use the estimated future state and the desired future state to determine control action. This control technique has been successfully applied to many different dynamic systems.

In standard linear model predictive control, the plant is modeled as a discrete linear system [4]. For the linear case when a finite horizon quadratic cost function is minimized, the optimal control sequence can be solved in closed form. When the plant is nonlinear, the optimal control sequence is, in general, not possible to obtain in closed form. However, in some special cases, closed-form optimal control sequences are possible. To solve these types of nonlinear optimal control problems requires difficult and laborious numerical optimization algorithms. An approach for solving the optimal problem was given by Chen and Allgöwer [5]. However, significant numerical computations are still required for all but the simplest cases and are not practical for real time implementation. Another approach is based on solving the state-dependent Riccati equation [6,7]. The state-dependent Riccati equation technique solves the

*Assistant Professor, Department of Mechanical and Aerospace Engineering. Member AIAA.

†Research Assistant, Department of Mechanical Engineering. Member AIAA.

‡Sikorsky Associate Professor, School of Aerospace Engineering. Associate Fellow AIAA.

nonlinear problem by satisfying the algebraic Riccati equation at each time step. However, this method also requires a significant amount of online iterative computations and is not feasible for many real time applications. Nonlinear model-based controllers with increased efficiency have been considered where predicted control moves are centered about an optimal control law. The predicted optimal control law is then continuously modified at future times to ensure an appropriate control [8–10]. This process allows the majority of computations to be calculated offline. Improvements on standard receding horizon controllers for nonlinear systems have been established by Magni et al. [11]. They demonstrated that using two distinct horizons, a prediction horizon and a shorter control horizon, can increase the domain of attraction for short control horizons. A suboptimal nonlinear model predictive control (NMPC) technique also has been proposed by Xin and Balakrishnan [12] that rewrites the original equation in a linearlike form and solves the Hamilton–Jacobi–Bellman equation by power series expansion; however, it is limited to control affine systems. Suboptimal NMPC techniques for nonaffine systems have been proposed by Patwardhan et al. [13] as well as Patwardhan and Madhavan [14]. An algorithm proposed by Rajendra et al. [15] works for nonaffine systems and requires less computation than other methods, but an iterative solution is required. An ideal NMPC algorithm displays the closed-form solution properties of linear MPC while being applicable to a wide range of nonlinear systems. Chen [16] developed a NMPC technique that can be applied to a general nonlinear plant by using Taylor expansion of the plant output and control. It is assumed that control weighting is not in the performance index and that control order is the difference between the Taylor series expansion and the relative degree of the system. This technique was developed for a general nonaffine single input single output system.

The work reported here presents a nonlinear model predictive control law in the same spirit as Chen’s algorithm except it is cast in a MIMO setting. After establishing the general algorithm it is specialized to air vehicles that are adequately described dynamically with a rigid 6-degrees-of-freedom representation. It is shown that a penalty for control can be implemented through the selection of the number of Taylor series expansion terms even with control being absent in the cost function. The methodology is successfully exercised on two systems, namely, a parafoil and payload aircraft along with a glider. Performance characteristics of the control strategy are presented through dynamic simulation results of both air vehicles.

II. Nonlinear Model Predictive Control Algorithm

Consider a general nonlinear system of the form as given in Eq. (1) with N inputs and P outputs. Notice that the assumed system is not affine in control.

$$\dot{\mathbf{x}} = f(\mathbf{x}, \mathbf{u}) \quad \mathbf{y} = h(\mathbf{x}) \quad (1)$$

For a nonlinear system, it is well known that after a specific number of derivatives of the output, control inputs appear. The relative degree M_i is the number of time derivatives of the i th output required for control to appear. When the control appears, it generally appears in a nonlinear manner. If successive time derivatives are obtained after the relative degree, time derivatives of control will also appear. Time derivatives of an output can be expressed as in Eq. (2) when the number of time derivatives of the output is less than M_i , where α_j^i is a function of only the state vector when j is less than the relative degree.

$$\frac{d^j y_i}{dt^j} = \alpha_j^i \quad (2)$$

Note that $\alpha_{M_i}^i$ is a function of both the state and the control. In general, when j is greater than the relative degree, the output can be expressed as in Eq. (3).

$$\frac{d^j y_i}{dt^j} = \alpha_j^i + \beta_{i1} \frac{d^{(M_i-j)} \dot{u}_1}{dt^{(M_i-j)}} + \dots + \beta_{iN} \frac{d^{(M_i-j)} \dot{u}_N}{dt^{(M_i-j)}} \quad (3)$$

Assume the input and output are sufficiently differentiable with respect to time so that the input equations can be approximated by a Taylor series of order R_i , where $R_i \geq M_i$. The output equations are approximated by Taylor series of order $S = R_i - M_i$, where each R_i is selected so that S is the same for all output equations.

$$y_i(t + \tau) \cong y_i(t) + \tau \frac{dy_i}{dt} + \dots + \frac{\tau^{R_i} d^{R_i} y_i}{R_i! dt^{R_i}} \quad (4)$$

$$u_i(t + \tau) \cong u_i(t) + \tau \frac{du_i}{dt} + \dots + \frac{\tau^S d^S u_i}{S! dt^S} \quad (5)$$

Rather than solving the control input function $u_i(t)$ over the control horizon, the control is parameterized with its S derivatives. Because $u_i(t)$ is not required to appear in the state equations in a linear manner, it can be considered to be a state variable. This converts determination of a continuous function for control into determination of a finite and relatively small number of discrete parameters to determine control. Subsequently this converts the resulting optimal control problem into a discrete parameter optimization problem. The parameters to be determined for the optimal control problem then become

$$U_i = \left[\frac{du_i}{dt} \quad \frac{d^2 u_i}{dt^2} \quad \dots \quad \frac{d^S u_i}{dt^S} \right]^T \quad (6)$$

$$\bar{U} = [U_1 \quad U_2 \quad \dots \quad U_N]^T \quad (7)$$

Assuming that parameters in Eq. (6) defining the control sequence are known, the control is expressed in Eq. (8).

$$u_i(t + \tau) \cong \int \left(\frac{du_i}{dt} + \tau \frac{d^2 u_i}{dt^2} + \dots + \frac{\tau^{S-1}}{(S-1)!} \frac{d^S u_i}{dt^S} \right) d\tau \quad (8)$$

In practical applications the control is only needed near the current time ($\tau = 0$). In this case, only the first derivative is required to determine the optimal control input.

$$u_i(t_2) \cong \frac{du_i}{dt} (t_2 - t_1) + u_i(t_1) \quad (9)$$

To develop compact expressions for the control input, the Taylor series expansion for the output in Eq. (4) are written in as

$$y_i(t + \tau) \cong T_i Y_i \quad (10)$$

$$T_i = \left[1 \quad \frac{\tau}{1!} \quad \frac{\tau^2}{2!} \quad \dots \quad \frac{\tau^{R_i}}{R_i!} \right] \quad (11)$$

$$Y_i = \left[y_i(t) \quad \frac{dy_i}{dt} \quad \dots \quad \frac{d^{R_i} y_i}{dt^{R_i}} \right]^T \quad (12)$$

Consider the entire output vector, approximated by a Taylor series up to order R_i (possibly different orders for each output).

$$y(t + \tau) \cong \begin{bmatrix} T_1 & 0 & \dots & 0 \\ 0 & T_2 & \ddots & \vdots \\ \vdots & \ddots & \ddots & 0 \\ 0 & \dots & 0 & T_p \end{bmatrix} \begin{Bmatrix} Y_1 \\ Y_2 \\ \vdots \\ Y_p \end{Bmatrix} = \bar{T} \bar{Y} \quad (13)$$

The matrix \bar{T} has dimensions of $[P \times V]$, where $V = \sum_{i=1}^N R_i$. The desired trajectory is approximated in the same manner.

$$y_D(t + \tau) \cong \bar{T} \bar{Y}_D \quad (14)$$

The tracking error can now be formed and expressed in compact notation

$$e(t + \tau) = \bar{Y}_D(t + \tau) - \bar{Y}(t + \tau) = \bar{T}(\bar{Y}_D - \bar{Y}) \quad (15)$$

In model predictive control, a quadratic cost function is minimized over a finite horizon.

$$\begin{aligned} J &= \frac{1}{2} \int_{T_1}^{T_2} e(t + \tau)^T Q e(t + \tau) d\tau \\ &= \frac{1}{2} \int_{T_1}^{T_2} (\bar{Y}_D - \bar{Y})^T \bar{T}^T Q \bar{T} (\bar{Y}_D - \bar{Y}) d\tau \end{aligned} \quad (16)$$

Tracking error cost is weighted with the possibly time-dependent positive definite matrix Q . Selecting the components of Q to be time varying allows initial or final tracking performance to be more heavily weighted. Because only \bar{T} , and possibly Q , depend on τ , the cost function can be rewritten in Eq. (17).

$$J = \frac{1}{2} (\bar{Y}_D - \bar{Y})^T \Pi (\bar{Y}_D - \bar{Y}) \quad (17)$$

The matrix Π_i is given in Eq. (18) for a constant diagonal Q matrix.

$$\begin{aligned} \Pi_i &= q_i \int_{T_1}^{T_2} T_i^T T_i d\tau \\ &= q_i \begin{bmatrix} \frac{t_2 - t_1}{(1)0!0!} & \frac{t_2^2 - t_1^2}{(2)0!1!} & \cdots & \frac{t_2^{R_i+1} - t_1^{R_i+1}}{(R_i+1)0!R_i!} \\ \frac{t_2^2 - t_1^2}{(2)1!0!} & \frac{t_2^3 - t_1^3}{(3)1!1!} & \cdots & \frac{t_2^{R_i+2} - t_1^{R_i+2}}{(R_i+2)1!R_i!} \\ \vdots & \vdots & \ddots & \vdots \\ \frac{t_2^{R_i+1} - t_1^{R_i+1}}{(R_i+1)R_i!0!} & \frac{t_2^{R_i+2} - t_1^{R_i+2}}{(R_i+2)R_i!1!} & \cdots & \frac{t_2^{2R_i+1} - t_1^{2R_i+1}}{(2R_i+1)R_i!R_i!} \end{bmatrix} \end{aligned} \quad (18)$$

$$\Pi = \begin{bmatrix} \Pi_1 & & & 0 \\ & \Pi_2 & & \\ & & \ddots & \\ 0 & & & \Pi_p \end{bmatrix} \quad (19)$$

Note that the matrix Π can be computed in closed form and stored. For the parameters \bar{U} to be an optimal solution, the cost function in Eqs. (17–19) must satisfy the gradient condition

$$\frac{\partial J}{\partial \bar{U}} = -(\bar{Y}_D - \bar{Y})^T \Pi \frac{\partial \bar{Y}}{\partial \bar{U}} = 0 \quad (20)$$

The optimal control input is determined by considering Eq. (20). Partition \bar{Y} , \bar{Y}_D , and $\partial \bar{Y} / \partial \bar{U}$ into upper and lower sections as shown in Eqs. (21–23).

$$\frac{\partial Y_i}{\partial U_j} = \begin{bmatrix} 0 & 0 & \cdots & 0 \\ 0 & 0 & & \vdots \\ \vdots & \vdots & \ddots & \\ 0 & 0 & \cdots & 0 \\ - & - & - & - \\ \beta_{i1} & 0 & 0 & 0 \\ \frac{\partial \alpha_{M_i+2}^i}{\partial u_j^1} & \beta_{i1} & 0 & 0 \\ \vdots & & \ddots & 0 \\ \frac{\partial \alpha_{R_i}^i}{\partial u_j^1} & \frac{\partial \alpha_{R_i}^i}{\partial u_j^2} & \cdots & \beta_{i1} \end{bmatrix} = \begin{Bmatrix} 0 \\ \beta_{i1}^* \end{Bmatrix} \quad (22)$$

$$\frac{\partial \bar{Y}}{\partial \bar{U}} = \begin{bmatrix} 0 & 0 & \cdots & 0 \\ \beta_{11}^* & \beta_{12}^* & \cdots & \beta_{1N}^* \\ 0 & 0 & \cdots & 0 \\ \beta_{21}^* & \beta_{22}^* & \cdots & \beta_{2N}^* \\ & & \vdots & \\ 0 & 0 & \cdots & 0 \\ \beta_{p1}^* & \beta_{p2}^* & \cdots & \beta_{pN}^* \end{bmatrix} \quad (23)$$

In a similar manner partition Π to be conformal with the vectors \bar{Y} and \bar{Y}_D .

$$\Pi = \begin{bmatrix} \Pi_{11}^1 & \Pi_{12}^1 & & & 0 \\ \Pi_{21}^1 & \Pi_{22}^1 & & & \\ & & \ddots & & \\ & & & \Pi_{11}^p & \Pi_{12}^p \\ 0 & & & \Pi_{21}^p & \Pi_{22}^p \end{bmatrix} \quad (24)$$

The format of $\partial \bar{Y} / \partial \bar{U}$ and Π allows for their multiplication to be written in compact form.

$$\begin{aligned} \Pi \frac{\partial \bar{Y}}{\partial \bar{U}} &= \begin{bmatrix} \Pi_{12}^1 & 0 & \cdots & 0 \\ \Pi_{22}^1 & 0 & \cdots & 0 \\ 0 & \Pi_{12}^2 & & \\ 0 & \Pi_{22}^2 & & \\ \vdots & \vdots & \ddots & \\ 0 & 0 & \Pi_{12}^p & \\ \cdots & & & \Pi_{22}^p \\ 0 & \cdots & 0 & \Pi_{22}^p \end{bmatrix} \begin{bmatrix} \beta_{11}^* & \beta_{12}^* & \cdots & \beta_{1N}^* \\ \beta_{21}^* & \beta_{22}^* & \cdots & \beta_{2N}^* \\ \vdots & \vdots & \ddots & \vdots \\ \beta_{p1}^* & \beta_{p2}^* & \cdots & \beta_{pN}^* \end{bmatrix} \\ &= \Pi_R dY \end{aligned} \quad (25)$$

With the selection of R_i such that the number of Taylor expansion terms in the control approximation for each control is equal and the

$$Y_i = \begin{Bmatrix} Y_i^U \\ Y_i^L \end{Bmatrix} = \begin{Bmatrix} \alpha_0^i(x) \\ \vdots \\ \alpha_{M_i-1}^i(x) \\ \alpha_{M_i}^i(x, u_{1-N}) \\ - \\ \alpha_{M_i+1}^i(x, u_{1-N}) + \beta_{i1}(x)\dot{u}_1 + \cdots + \beta_{iN}(x)\dot{u}_N \\ \vdots \\ \alpha_{R_i}^i(x, u_{1-N}, \dots, d^{(S-1)}u_{1-N}/dt^{(S-1)}) + \beta_{i1}(x)\frac{d^S u_1}{dt^S} + \cdots + \beta_{iN}(x)\frac{d^S u_N}{dt^S} \end{Bmatrix} \quad (21)$$

system is square, i.e., the number of inputs and outputs are equal, dY is a square $S \times P$ matrix and Π_R has dimensions of $(V + P) \times (S \times P)$. The equivalent optimal condition is then expressed as follows.

$$(\bar{Y}_D - \bar{Y})^T \Pi_R dY = 0 \quad (26)$$

Where dY^{-1} exists, we have the following condition.

$$(\bar{Y}_D - \bar{Y})^T \Pi_R = 0 \quad (27)$$

Because of the block structure Π_R can be expanded as in Eq. (28). The resulting P conditions for optimality are shown in Eq. (29).

$$\left(\begin{Bmatrix} Y_{Di}^U \\ Y_{Di}^L \end{Bmatrix} - \begin{Bmatrix} Y_i^U \\ Y_i^L \end{Bmatrix} \right)^T \begin{Bmatrix} \Pi_{12} \\ \Pi_{22} \end{Bmatrix} = [0] \quad (28)$$

$$Y_i^L = (\Pi_{22}^L)^{-1} (\Pi_{12}^L)^T (Y_{Di}^U - Y_i^U) + Y_{Di}^L \quad (29)$$

If we are interested only in the current control input, then \dot{u} is the only derivative required which is the first component of Y_i^L . Denoting the first row of $(\Pi_{22}^L)^{-1} (\Pi_{12}^L)^T$ as K_i and evaluating the first component of Y_i^L the optimal solution for the first time derivative of the control u is given in Eqs. (30–37).

$$B = \begin{bmatrix} \beta_{11} & \cdots & \beta_{1N} \\ \vdots & \ddots & \vdots \\ \beta_{P1} & \cdots & \beta_{PN} \end{bmatrix} \quad (30)$$

$$A = [\alpha_{M_1+1}^1 \quad \cdots \quad \alpha_{M_P+1}^N]^T \quad (31)$$

$$Y_D^L = [Y_{D1}^L(1) \quad \cdots \quad Y_{DP}^L(1)]^T \quad (32)$$

$$Y_D^U = \begin{bmatrix} Y_{D1}^U \\ \vdots \\ Y_{DP}^U \end{bmatrix} \quad (33)$$

$$Y^U = \begin{bmatrix} Y_1^U \\ \vdots \\ Y_P^U \end{bmatrix} \quad (34)$$

$$U_C = [\dot{u}_1(t) \quad \cdots \quad \dot{u}_N(t)]^T \quad (35)$$

$$K = \begin{bmatrix} K_1 & 0 & \cdots & 0 \\ 0 & K_2 & \ddots & \vdots \\ \vdots & \ddots & \ddots & 0 \\ 0 & \cdots & 0 & K_P \end{bmatrix} \quad (36)$$

Using this notation, the MIMO control law is

$$U_C = B^{-1} [K_T (Y_D^U - Y^U) + Y_D^L - A] \quad (37)$$

In the case of a SISO system, Eq. (37) reduces to the following scalar result for the optimal control derivative (13).

$$\dot{u} = \frac{1}{\beta_{M+1}} \left(K (Y_D^U - Y^U) + \frac{d^{M+1} y_D}{dt^{M+1}} - \alpha_{M+1} \right) \quad (38)$$

III. Application to a Rigid Air Vehicle Model

Many air vehicles can be modeled as a rigid body possessing six degrees of freedom (DOF) including three inertial position components of the system mass center as well as the three Euler orientation angles. Kinematic equations of motion for the general system are provided in Eqs. (39) and (40).

$$\begin{Bmatrix} \dot{x}_I \\ \dot{y}_I \\ \dot{z}_I \end{Bmatrix} = R_{IB}^T \begin{Bmatrix} u_b \\ v_b \\ w_b \end{Bmatrix} \quad (39)$$

$$\begin{Bmatrix} \dot{\phi} \\ \dot{\theta} \\ \dot{\psi} \end{Bmatrix} = \begin{bmatrix} 1 & s_\phi t_\theta & c_\phi t_\theta \\ 0 & c_\phi & -s_\phi \\ 0 & s_\phi / c_\theta & c_\phi / c_\theta \end{bmatrix} \begin{Bmatrix} p \\ q \\ r \end{Bmatrix} = K_{RM} \omega \quad (40)$$

The matrix R_{IB} represents the transformation matrix from an inertial reference frame to the body reference frame.

$$R_{IB} = \begin{bmatrix} c_\theta c_\phi & c_\theta s_\phi & -s_\theta \\ s_\phi s_\theta c_\psi - c_\phi s_\psi & s_\phi s_\theta s_\psi + c_\phi c_\psi & c_\theta s_\phi \\ c_\phi s_\theta c_\psi + s_\phi s_\psi & c_\phi s_\theta s_\psi - s_\phi c_\psi & c_\phi c_\theta \end{bmatrix} \quad (41)$$

The common shorthand notation for trigonometric functions is employed where $\sin(\alpha) \equiv s_\alpha$, $\cos(\alpha) \equiv c_\alpha$, and $\tan(\alpha) \equiv t_\alpha$. The dynamic equations of motion are provided in Eqs. (42) and (43).

$$\begin{Bmatrix} \dot{u}_b \\ \dot{v}_b \\ \dot{w}_b \end{Bmatrix} = \frac{1}{m} \begin{Bmatrix} X \\ Y \\ Z \end{Bmatrix} + g \begin{Bmatrix} -s_\phi \\ s_\phi c_\theta \\ c_\phi c_\theta \end{Bmatrix} - \begin{bmatrix} 0 & -r & q \\ r & 0 & -p \\ -q & p & 0 \end{bmatrix} \begin{Bmatrix} u_b \\ v_b \\ w_b \end{Bmatrix} \quad (42)$$

$$\begin{Bmatrix} \dot{p} \\ \dot{q} \\ \dot{r} \end{Bmatrix} = I^{-1} \left(\begin{Bmatrix} L \\ M \\ N \end{Bmatrix} - \begin{bmatrix} 0 & -r & q \\ r & 0 & -p \\ -q & p & 0 \end{bmatrix} I_T \begin{Bmatrix} p \\ q \\ r \end{Bmatrix} \right) \quad (43)$$

Where

$$\begin{Bmatrix} X \\ Y \\ Z \end{Bmatrix} = \frac{1}{2} \rho S_R V_A^2 (F_A + F_C u) \quad (44)$$

$$\begin{Bmatrix} L \\ M \\ N \end{Bmatrix} = \frac{1}{2} \rho S_R V_A^2 (M_A + M_C u) \quad (45)$$

$$\begin{Bmatrix} \dot{L} \\ \dot{M} \\ \dot{N} \end{Bmatrix} = \rho S_R V_A \dot{V}_A (M_A + M_C u) + \frac{1}{2} \rho S_R V_A^2 (\dot{M}_A + \dot{M}_C u + M_C \dot{u}) \quad (46)$$

A common goal of air vehicles is to track desired roll, pitch, and yaw angles. The output for an angle tracking controller is given in Eq. (47).

$$y = [\phi \quad \theta \quad]^T \quad (47)$$

The relative degree of each output is 2; therefore three derivatives of the output equations are required. The first derivative of the output is Eq. (40), the second derivative is not shown, and the third derivative follows:

$$\ddot{y} = 2\dot{K}_{RM}\dot{\omega} + K_{RM}\ddot{\omega} + \ddot{K}_{RM}\omega \quad (48)$$

The matrix B in Eq. (30) and the vector A in Eq. (31) are found to be

$$A = 2\dot{K}_{RM}\dot{\omega} + \ddot{K}_{RM}\omega + K_{RM}I^{-1} \left(\rho S_R V_A \dot{V}_A (M_A + M_C u) + \frac{1}{2} \rho S_R V_A^2 (\dot{M}_A + \dot{M}_C u) - S_\omega I \omega - S_\omega I \dot{\omega} \right) \quad (49)$$

$$B = \frac{1}{2} \rho S_R V_A^2 K_{RM} I^{-1} M_C \quad (50)$$

Using Eqs. (48) and (49) we can solve for the desired control derivatives by substitution into Eq. (37).

$$\begin{aligned}
U_C = & \frac{2}{\rho S_R V_A^2} M_C^{-1} \left(I K_{RM}^{-1} [Y_D^{L1} + K(Y_D^U - Y^U) - 2\dot{K}_{RM}\dot{\omega} - \ddot{K}_{RM}\omega] \right. \\
& - \rho S_R V_A \dot{V}_A (\mathbf{M}_A + M_C \mathbf{u}) - \frac{1}{2} \rho S_R V_A^2 (\dot{\mathbf{M}}_A + \dot{M}_C \mathbf{u}) \\
& \left. + S_{\dot{\omega}} \mathbf{I} \omega + S_{\omega} \mathbf{I} \dot{\omega} \right) \quad (51)
\end{aligned}$$

The matrices S_{ω} and $S_{\dot{\omega}}$ are the skew-symmetric cross product operators on ω and $\dot{\omega}$, respectively. The quantities F_A and F_C which include aerodynamic force coefficients do not directly appear in Eq. (51) but will enter in through \dot{V}_A . Two matrix inversions are required in the control law and fortunately one is easily determined in closed form:

$$K_{RM}^{-1} = \begin{bmatrix} -s_{\theta} & 0 & 1 \\ s_{\phi} c_{\theta} & c_{\phi} & 0 \\ c_{\theta} c_{\phi} & -s_{\phi} & 0 \end{bmatrix} \quad (52)$$

It is clear from Eq. (51) that the optimal control derivatives U_C are valid for a general rigid air vehicle where only the force and moment equations depend on the specific system. The optimal control derivatives U_C can be found for a specific system provided that aerodynamic expressions for F_A , F_C , M_A , and M_C are known.

Because of the symmetry of the parafoil system the inertia matrix takes the form

$$I = \begin{bmatrix} I_{XX} & 0 & I_{XZ} \\ 0 & I_{YY} & 0 \\ I_{XZ} & 0 & I_{ZZ} \end{bmatrix} \quad (55)$$

$$I^{-1} = \begin{bmatrix} I_{XXI} & 0 & I_{XZI} \\ 0 & I_{YYI} & 0 \\ I_{XZI} & 0 & I_{ZZI} \end{bmatrix} \quad (56)$$

For a SISO system the control derivatives are given in Eq. (38). The parafoil system has relative degree of 2, requiring three derivatives of the output equation to find α_3 and β_3 . Taking the three derivatives of the output and writing \dot{L} , \dot{M} , and \dot{N} in compact form, \ddot{y} can be written in the desired form of Eq. (3) with α_3 and β_3 given in Eqs. (60) and (61).

$$\begin{Bmatrix} \dot{L} \\ \dot{M} \\ \dot{N} \end{Bmatrix} = \begin{Bmatrix} \dot{L}_{\alpha} \\ \dot{M}_{\alpha} \\ \dot{N}_{\alpha} \end{Bmatrix} + \begin{Bmatrix} \dot{L}_{\beta} \\ \dot{M}_{\beta} \\ \dot{N}_{\beta} \end{Bmatrix} \ddot{u} \quad (57)$$

$$\begin{Bmatrix} \dot{L}_{\alpha} \\ \dot{M}_{\alpha} \\ \dot{N}_{\alpha} \end{Bmatrix} = \frac{1}{2} \rho S_R \begin{Bmatrix} 2V_A \dot{V}_A C_{l\phi} b \dot{\phi} + V_A^2 C_{lp} b \dot{\phi} + \frac{\dot{V}_A C_{lp} b^2 p}{2} + \frac{V_A C_{lp} b^2 \dot{p}}{2} + \frac{2V_A \dot{V}_A C_{l\delta_a} b \delta_a}{d} \\ 2V_A \dot{V}_A C_{m0} c + 2V_A \dot{V}_A C_{m\alpha} \alpha + V_A^2 C_{m\alpha} \dot{\alpha} + \frac{\dot{V}_A C_{mq} c^2 q}{2} + \frac{V_A C_{mq} c^2 \dot{q}}{2} \\ \frac{\dot{V}_A C_{nr} b^2 r}{2} + \frac{V_A C_{nr} b^2 \dot{r}}{2} + \frac{2V_A \dot{V}_A C_{n\delta_a} b \delta_a}{d} \end{Bmatrix} \quad (58)$$

$$\begin{Bmatrix} \dot{L}_{\beta} \\ \dot{M}_{\beta} \\ \dot{N}_{\beta} \end{Bmatrix} = \frac{\rho S_R b}{2d} \begin{Bmatrix} V_A^2 C_{l\delta_a} \\ 0 \\ V_A^2 C_{n\delta_a} \end{Bmatrix} \quad (59)$$

$$\begin{aligned}
\alpha_3 = & \left(\frac{1}{c_{\theta}} \right) \left(-S_{\phi} \dot{\phi}^2 q + c_{\phi} \ddot{\phi} q + 2c_{\phi} \dot{\phi} \dot{q} + \frac{\dot{\theta}^2 S_{\phi} q}{c_{\theta}^2} + t_{\theta} \ddot{\theta} S_{\phi} q + t_{\theta} \dot{\theta} c_{\phi} \dot{\phi} q + t_{\theta} \dot{\theta} S_{\phi} \dot{q} - c_{\phi} \dot{\phi}^2 r - S_{\phi} \ddot{\phi} r - 2S_{\phi} \dot{\phi} \dot{r} + \frac{\dot{\theta}^2 c_{\phi} r}{c_{\theta}^2} + t_{\theta} \ddot{\theta} c_{\phi} r - t_{\theta} \dot{\theta} S_{\phi} \dot{r} \right. \\
& \left. + t_{\theta} \dot{\theta} c_{\phi} \dot{r} \right) + \left(\frac{t_{\theta} \dot{\theta}}{c_{\theta}} \right) (c_{\phi} \dot{\phi} q + S_{\phi} \dot{q} + t_{\theta} \dot{\theta} S_{\phi} q - S_{\phi} \dot{r} + c_{\phi} \dot{r} + t_{\theta} \dot{\theta} c_{\phi} r) + \left(\frac{c_{\phi}}{c_{\theta}} \right) \{ I_{XZI} [\dot{L}_{\alpha} + (I_{YY} - I_{ZZ})(\dot{q}r + q\dot{r}) - I_{XZ}(\dot{p}q + p\dot{q})] \\
& + I_{ZZI} [\dot{N}_{\alpha} + (I_{XX} - I_{YY})(\dot{p}q + p\dot{q}) + I_{XZ}(\dot{q}r + q\dot{r})] \} + \left(\frac{S_{\phi}}{c_{\theta}} \right) I_{YYI} [\dot{M}_{\alpha} + (I_{ZZ} - I_{XX})(\dot{p}r + p\dot{r}) + 2I_{XZ}(p\dot{p} - r\dot{r})] \quad (60)
\end{aligned}$$

IV. Parafoil and Payload Aircraft Application

A parafoil and payload controlled by left and right parafoil brake deflection can be modeled as a SISO system where heading angle is the output and asymmetric brake deflection δ_a is the control. The parafoil and payload shown in Fig. 1 can be represented as a 6-DOF system with aerodynamic forces acting at the total system mass center and aerodynamic moments about the system mass center. The aerodynamic loads are given in Eqs. (53) and (54). Apparent mass effects which become negligible in near steady-state conditions have been neglected [17].

$$\begin{aligned}
\begin{Bmatrix} X \\ Y \\ Z \end{Bmatrix} = & \frac{1}{2} \rho S_R V_A (C_{L0} + C_{L\alpha} \alpha) \begin{Bmatrix} w_a \\ 0 \\ -u_a \end{Bmatrix} - \frac{1}{2} \rho S_R V_A (C_{D0} + C_{D\alpha} \alpha^2 \\
& + C_{D\delta_a} \delta_a) \begin{Bmatrix} u_a \\ v_a \\ w_a \end{Bmatrix} \quad (53)
\end{aligned}$$

$$\begin{Bmatrix} L \\ M \\ N \end{Bmatrix} = \frac{1}{2} \rho S_R V_A^2 \left[\begin{Bmatrix} C_{l\phi} b \dot{\phi} + \frac{C_{lp} b^2 p}{2V_A} \\ C_{m0} c + C_{m\alpha} \alpha + \frac{C_{mq} c^2 q}{2V_A} \\ \frac{C_{nr} b^2 r}{2V_A} \end{Bmatrix} + \begin{Bmatrix} \frac{C_{l\delta_a} b}{d} \\ 0 \\ \frac{C_{n\delta_a} b}{d} \end{Bmatrix} \delta_a \right] \quad (54)$$

$$\beta_3 = \left(\frac{c_{\phi}}{c_{\theta}} \right) (I_{XZI} \dot{L}_{\beta} + I_{ZZI} \dot{N}_{\beta}) + \left(\frac{S_{\phi}}{c_{\theta}} \right) I_{YYI} \dot{M}_{\beta} \quad (61)$$

The optimal solution for the first time derivative of the control δ_a given in Eq. (38) is now found for the parafoil and payload system. For δ_a to be finite it must be verified that β_3 is not zero throughout the expected flight envelope, i.e., the roll angle ϕ must not be $\pm\pi/2$ and \dot{L}_{β} , \dot{M}_{β} , and \dot{N}_{β} are not all zero. It is clear from Eq. (59) that two conditions could make \dot{L}_{β} and \dot{N}_{β} zero: V_A being equal to zero and the aerodynamic control coefficients $C_{l\delta_a}$ and $C_{n\delta_a}$ both equal to zero. Both cases correspond to the parafoil being uncontrollable.

To exercise the preceding algorithm for an example parafoil and payload system, the preceding system of equations describing the parafoil and payload aircraft are numerically integrated using a fourth-order Runge-Kutta algorithm to generate trajectories of the system. Simulations under different conditions are generated so that performance of the nonlinear model predictive controller can be evaluated. The physical parameters used for the parafoil and payload aircraft in simulations are provided in Table 1, whereas the aerodynamic coefficients are provided in Table 2. In all results presented, it is assumed that the control δ_a is updated every 0.01 s.

The accuracy of the approximation of the output and control sequence is determined by the number of terms in the Taylor expansion which is R for the output equation and $S = R - M$ for the control sequence. The accuracy of the approximations can then be defined to arbitrary accuracy in theory by choosing R arbitrarily

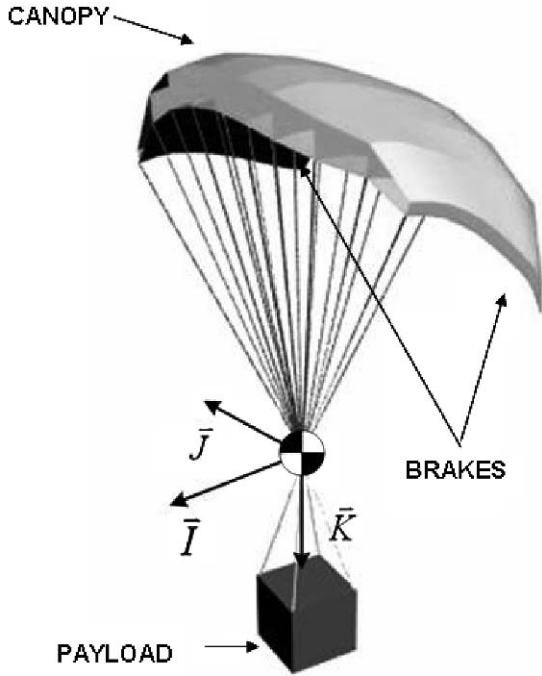


Fig. 1 Parafoil and payload.

large. In practice, however, the size of R and S are limited by the conditioning of the matrix Π_{22} whose inverse must be calculated to find the gains used in the control sequence given in Eq. (38). Notice that Π_{22} is independent of the plant and output and depends only on the prediction horizon, relative degree, and the number of expansion terms used in the control equation approximation. Hence, conditioning of Π_{22} is also independent of the plant and output. For this case the practical limit on S is near 8, at which point Π_{22} becomes severely ill conditioned. The selection of S can also be understood by inspection of the control approximation in Eqs. (5) and (6). If R is selected small and equal to one more than the relative degree, $S = 1$, the optimal control problem reduces to limiting the desired control to be linear over the entire prediction horizon. This limitation causes a

Table 1 Parafoil and payload physical parameters

Variable	Value	Units
ρ	0.00238	slug \times ft ³
Weight	50.0	lbf
S	72.0	ft ²
b	12.0	ft
c	6.0	ft
d	2.0	ft
I_{XX}	4.83	slug \times ft ²
I_{YY}	5.31	slug \times ft ²
I_{ZZ}	2.22	slug \times ft ²
I_{XZ}	0.0006	slug \times ft ²
I_{XY}, I_{YZ}	0.0006	slug \times ft ²

Table 2 Parafoil and payload aerodynamic coefficients

Parameter	Value
C_{L0}	0.400
$C_{L\alpha}$	2.000
C_{D0}	0.150
C_{Da^2}	1.000
$C_{D\delta_a}$	0.001
$C_{l\phi}$	-0.050
C_{lp}	-0.100
$C_{l\delta_a}$	0.002
C_{nr}	-0.070
$C_{n\delta_a}$	0.004

conservative solution for control. In contrast, as R is increased so that S is large, the expansion approximation can represent large and rapidly varying control and the solution for the optimal control approaches infinity because no penalty of the control exists in the cost function. The number of control expansion terms can then be viewed as a penalty term for control, where large S corresponds to low control penalty and a small S corresponds to large control penalty.

Figures 2 and 3 show simulation results for the parafoil and payload system tracking a constant heading of 45 deg where the prediction horizon is held constant at 3 s beginning with t_1 being zero and S is increased from 1 to 6. As S is increased the limitation on the control is decreased and the tracking performance becomes better. It can also be seen that as S becomes large the control sequence does indeed become more severe and if S could be chosen arbitrarily large the control sequence would approach initial impulse control achieving near perfect tracking at the cost of a large control input.

Figures 4 and 5 show a comparison of increasing control horizon with a fixed number of six expansion terms. In Fig. 4 it is clear that as the prediction horizon is increased tracking performance is decreased. As the prediction horizon is increased the Taylor series expansion must approximate a longer range of both the output and control sequence. For extension of the prediction horizon to achieve better tracking performance, the number of Taylor series expansion terms must also be increased so as to maintain an adequate level of control and output approximation over the extended horizon.

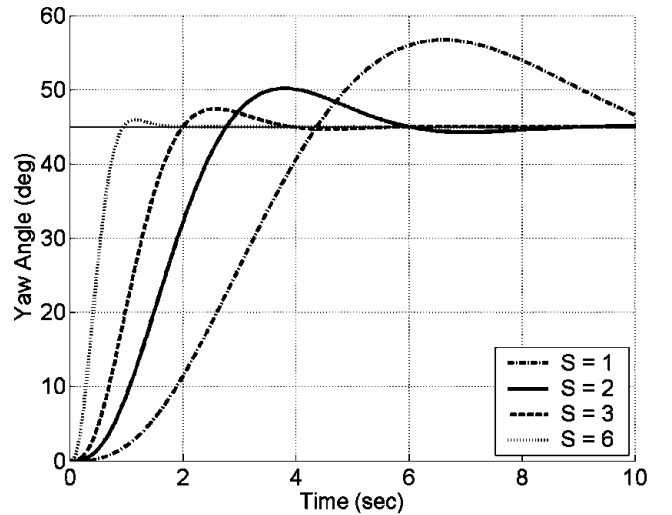


Fig. 2 Yaw angle for constant control horizon ($t_2 = 3.0, t_1 = 0.0$).

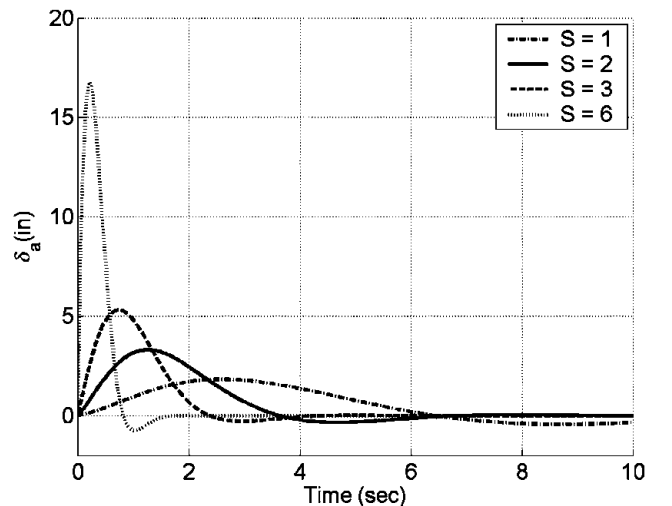


Fig. 3 Control history for constant control horizon ($t_2 = 3.0, t_1 = 0.0$).

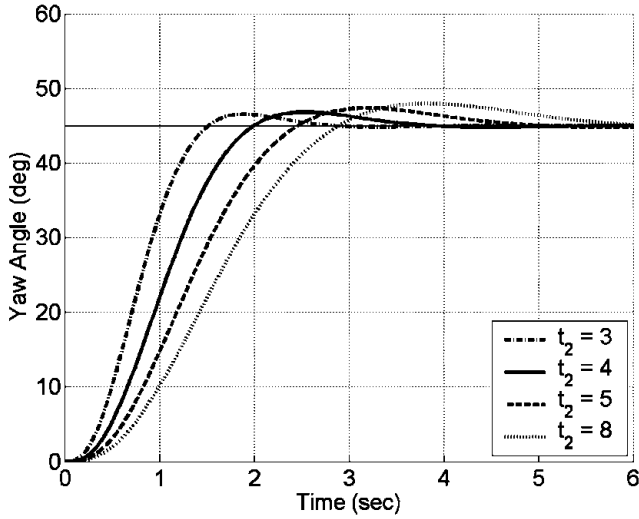


Fig. 4 Yaw angle for constant expansion order ($S = 4, t_1 = 0.0$).

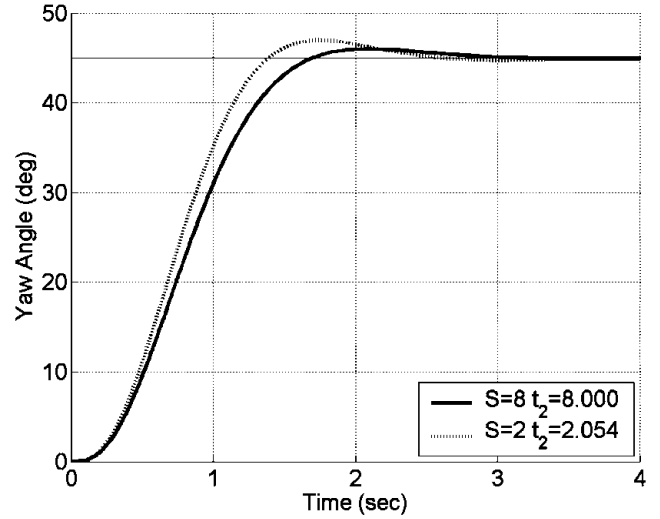


Fig. 6 Yaw angle for comparison of similar control gains ($t_1 = 0.0$).

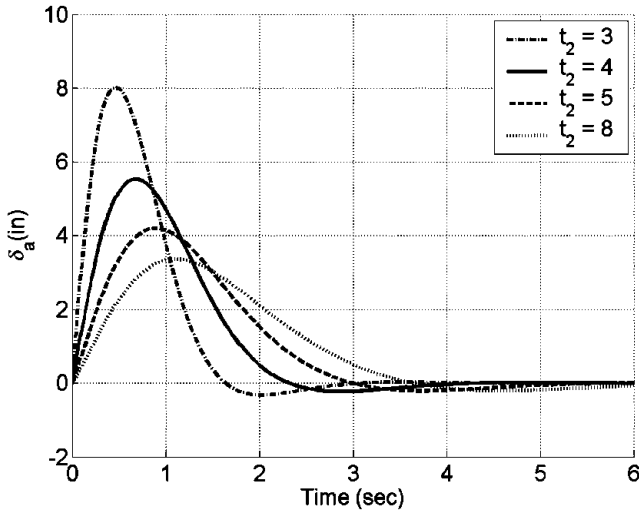


Fig. 5 Control for constant expansion order ($S = 4, t_1 = 0.0$).

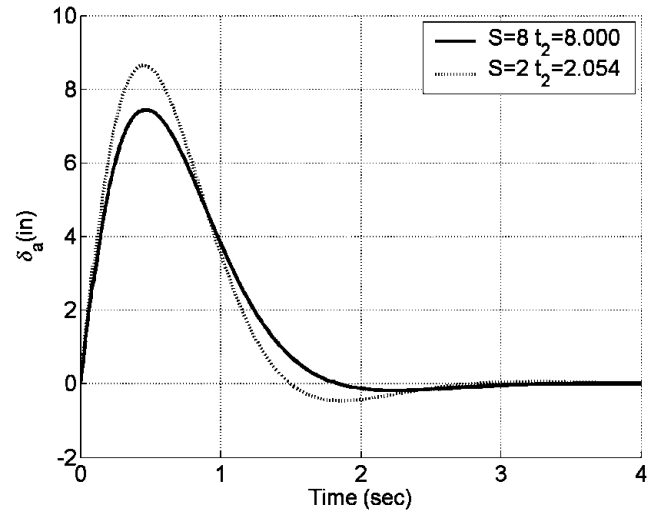


Fig. 7 Control for comparison of similar control gains ($t_1 = 0.0$).

As the prediction horizon becomes large so must S , but as already mentioned, the size of S is limited by R and the conditioning of Π_{22} . This problem can be circumvented because the optimal control gains in the vector K for large prediction horizon and large S can be approximated by a smaller prediction horizon and smaller S . Figures 6 and 7 show a comparison of a larger prediction horizon of 8.0 s with $S = 8$ and a smaller prediction horizon of 2.054 s with $S = 3$. The gain vector K for the larger prediction horizon is

$$\{25.59 \quad 20.47 \quad 7.00\}$$

whereas the gain vector K for the smaller prediction horizon is

$$\{29.08 \quad 20.47 \quad 6.57\}$$

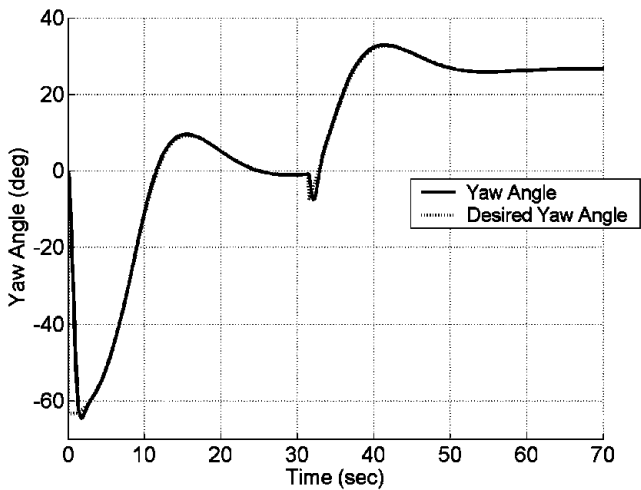
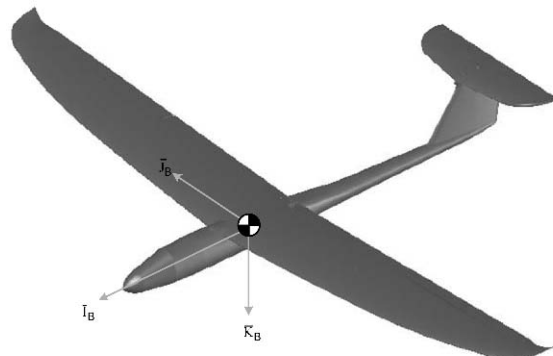
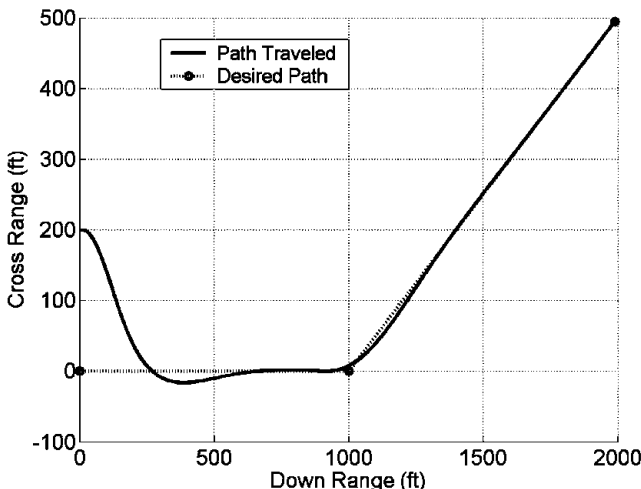
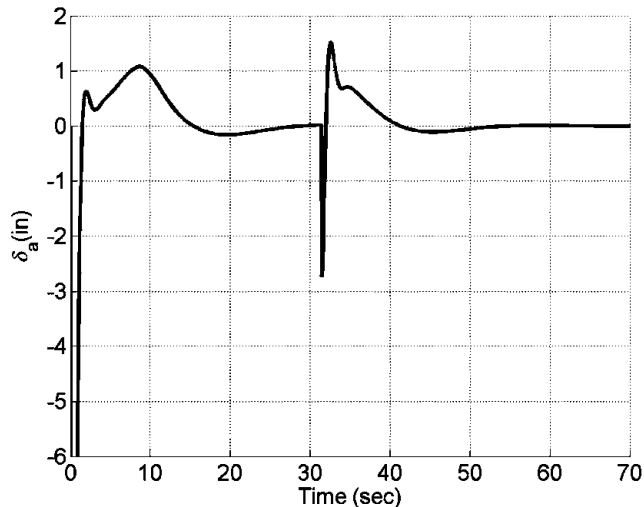
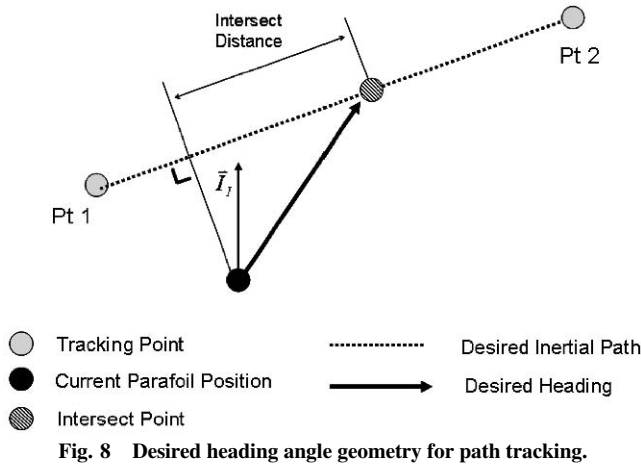
Figure 6 shows that the tracking performance and gain vectors are similar for the two cases. If a large prediction horizon is desired that requires too large a value of S , a nearly equivalent set of gains can be found by selecting a smaller S and an appropriate prediction horizon. This implies that two possible methods can be used in selecting the prediction horizon and the number of control expansion terms S . The first method: select a desired prediction horizon specific to the plant and then choose S to achieve an appropriate penalty on the control sequence. The second method: if S cannot be chosen large enough in the first method, then a nearly equivalent NMPC can be designed by selecting S as large as reasonable so that the matrix Π_{22} is well

conditioned and then choosing an appropriate prediction horizon so as to achieve a suitable control penalty.

Often tracking a desired heading angle is an intermediate step to a more complicated control problem such as tracking a desired path in inertial space. One approach is to convert the path into a desired heading angle and rates of change of the desired heading angle. Figure 8 shows geometry used to convert a desired path defined by two points into a desired heading. A parameter called the “intersect distance” is used along with two tracking points and the current position to define a desired heading. The current and previous desired heading angles are used to estimate the time derivatives of the desired heading angle. A desired heading and the first time derivative of desired heading with an intersect distance of 100 ft are used with the nonlinear model predictive strategy described in Sec. III. A prediction horizon of 2.054 s and $S = 3$ are used and provide a gain vector K of

$$\{29.08 \quad 20.47 \quad 6.57\}$$

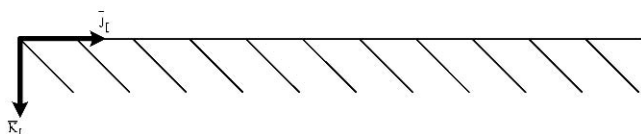
Figure 9 shows the performance of control strategy for a desired path defined by three tracking points: (0 ft, 0 ft), (1000 ft, 0 ft), and (2000 ft, 500 ft). The parafoil is initially at (200 ft, 0 ft) but quickly reaches the desired path near 250 ft down range. Figure 10 shows the desired heading angle and actual heading angle where the only significant control error is at the initial location and at 33 seconds where the turn at 1000 ft downrange is reached. The control is shown



in Fig. 11 where the largest control occurs initially and when the turn is reached.

V. Glider Application

An angle tracking controller for a glider shown in Fig. 12 is considered with the output vector given in Eq. (47). The controls are given in Eq. (62) where δ_a , δ_f , and δ_e are the aileron, flaps, and elevator controls, respectively.



$$\mathbf{u} = \{ \delta_a \quad \delta_f \quad \delta_e \}^T \quad (62)$$

The glider aerodynamic forces and moment coefficient quantities required in Eq. (51) are provided in Eqs. (63–66).

$$\mathbf{F}_A = \left\{ \begin{array}{l} C_{x0} + C_{x\alpha}\alpha + (c/V_A)C_{xq}q \\ C_{y\beta}\beta + (b/2V_A)(C_{yp}p + C_{yr}r) \\ C_{z0} + C_{z\alpha}\alpha + (c/V_A)C_{zq}q \end{array} \right\} \quad (63)$$

$$[\mathbf{F}_C] = \begin{bmatrix} C_{x\delta_e} & C_{x\delta_f} & 0 \\ 0 & 0 & C_{y\delta_a} \\ C_{z\delta_e} & C_{z\delta_f} & 0 \end{bmatrix} \quad (64)$$

$$\mathbf{M}_A = \left\{ \begin{array}{l} \left(\frac{b}{2} \right) \left(C_{L\beta}\beta + \frac{bC_{Lp}p}{2V_A} + \frac{bC_{Lr}r}{2V_A} \right) \\ c \left(C_{M0} + C_{M\alpha}\alpha + \frac{cC_{Mq}q}{V_A} \right) \\ \left(\frac{b}{2} \right) \left(C_{N\beta}\beta + \frac{bC_{Np}p}{2V_A} + \frac{bC_{Nr}r}{2V_A} \right) \end{array} \right\} \quad (65)$$

$$[\mathbf{M}_C] = \begin{bmatrix} \frac{dC_{L\delta_a}}{2} & 0 & 0 \\ 0 & cC_{M\delta_f} & cC_{M\delta_e} \\ \frac{bC_{N\delta_a}}{2} & 0 & 0 \end{bmatrix} \quad (66)$$

Table 3 Glider physical properties

Variable	Value	Units
ρ	0.00238	slug \times ft ³
Weight	1.99	lbf
S	4.35	ft ²
b	5.50	ft
c	0.557	ft
I_{XX}	0.0548	slug \times ft ²
I_{YY}	0.0288	slug \times ft ²
I_{ZZ}	0.0813	slug \times ft ²
I_{XZ}	$-5.78e - 005$	slug \times ft ²
I_{XY}	$-5.05e - 006$	slug \times ft ²
I_{YZ}	$-1.93e - 006$	slug \times ft ²

Table 4 Glider airfoil parameters

Main wing airfoil	RG-15
Main wing flaps	Trailing edge individual control
T-tail airfoil	NACA 0009
T-tail flaps	Trailing edge elevator only

The matrix M_c contains the systems control moment coefficients and may in general be singular. In the glider considered, the elevator and flap controls are redundant with respect to control moments, therefore the coefficient matrix is singular. In this case the pseudoinverse may be used in the optimal control solution to find the best fit solution.

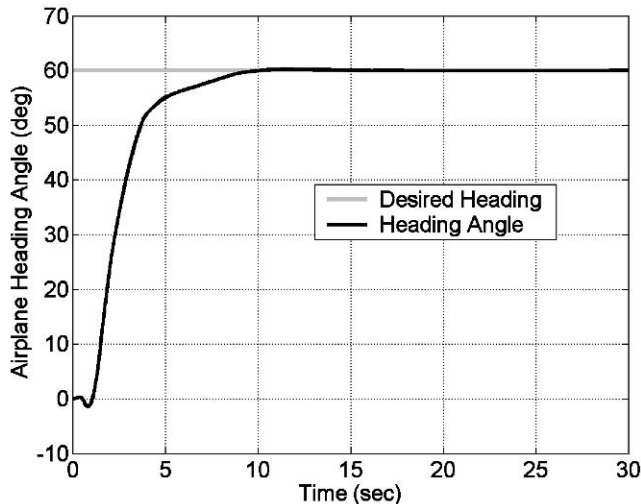
The preceding system of equations describing the rigid glider are numerically integrated using a fourth-order Runge–Kutta algorithm to generate trajectories of the system. One example scenario is examined using the physical parameters provided in Table 3, and the aerodynamic properties provided in Table 4. In the following results, the control derivative is updated every 0.01 s.

Figures 13–16 show simulation results for the glider tracking a constant heading angle of 60 deg, roll angle of 0.34 times the heading angle error, and a pitch angle of $22.5 \sin(t) - 6$ deg. The values

$$\begin{bmatrix} 1 & 2 & 1 \end{bmatrix}$$

are used in the error weighting matrix, the control is approximated with an eighth-order Taylor series expansion, and the prediction horizon is 1.0–6.0 s.

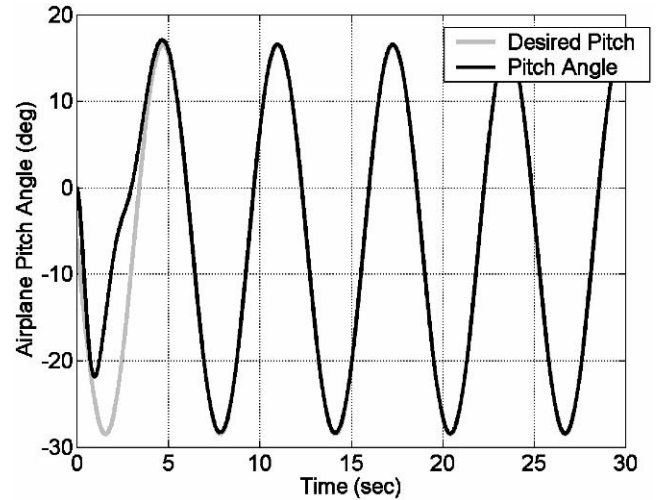
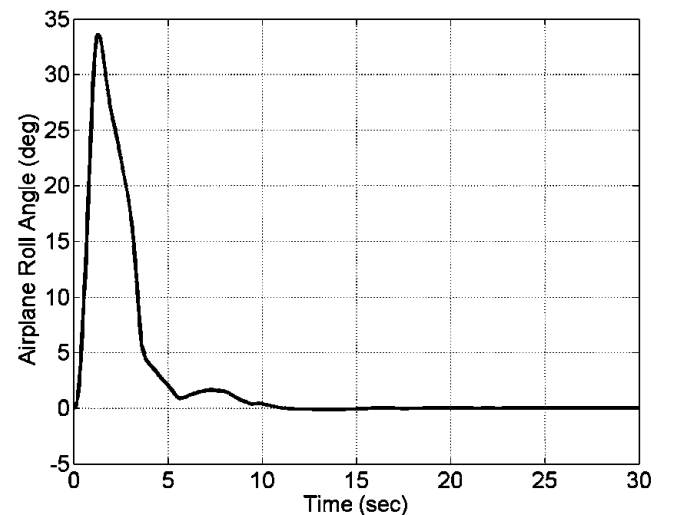
As in the parafoil case, the prediction horizon and Taylor series expansion orders are used to balance control magnitude and tracking error. Heading angle and pitch angle converge to their desired values within 7 s. To allow a more aggressive time varying pitch trajectory

**Fig. 13 Glider heading angle time history.**

to be easily tracked, a constant weighing factor of 2 is applied to the pitch angle error compared to unity for both the heading and roll angle errors.

VI. Conclusions

A nonlinear model predictive control strategy for tracking a desired orientation trajectory was developed for a general rigid air vehicle. The control strategy was simulated for an autonomous parafoil and payload system and an autonomous glider. The performance of the controller was evaluated by varying prediction horizons and number of Taylor expansion terms used for the approximation of the output equation and the control sequence. It was observed that a penalty for control can be implemented through the selection of the number of Taylor series expansion terms even with control being absent in the cost function. The selection of the number of terms in the Taylor series expansion was limited only by the conditioning of the matrix Π_{22} . Also, the limitation on the size of S can be circumvented because a nearly equivalent controller to that for a large S and large prediction horizon can be found for a small S with the appropriate prediction horizon. This observation leads to two possible methods for selecting S and the prediction horizon. The first method: select a desired prediction horizon specific to the plant and then choose S to achieve an appropriate penalty on the control sequence. The second method: if S cannot be chosen large enough in the first method, then a nearly equivalent controller can be designed by selecting S as large as reasonable so that the matrix Π_{22} is well

**Fig. 14 Glider pitch angle time history.****Fig. 15 Glider bank angle time history.**

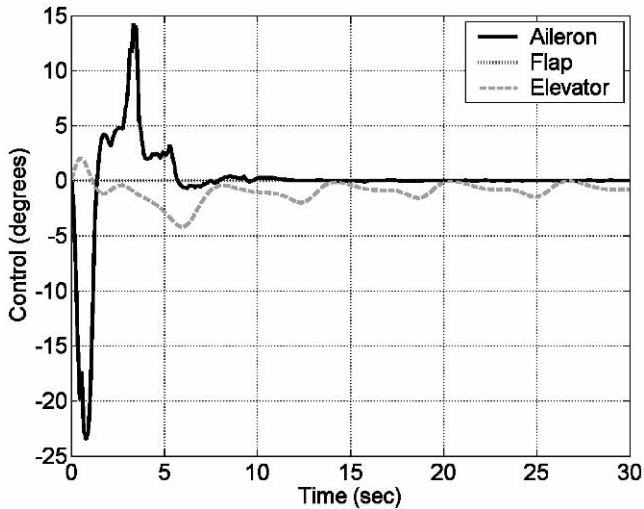


Fig. 16 Glider control deflection time history.

conditioned and then choosing an appropriate prediction horizon so as to achieve a suitable control penalty. Another more complex example is reported for an autonomous glider system in which elevator and flap controls were redundant. The redundancy made the control matrix M_C singular. It was successfully demonstrated that a pseudoinverse can be used.

References

- [1] Dogan, A., and Venkataramanan, S., "Nonlinear Control for Reconfiguration of Unmanned-Aerial-Vehicle Formation," *Journal of Guidance, Control, and Dynamics*, Vol. 28, No. 4, 2005, pp. 667–678.
- [2] Chaudhuri, A., and Seetharama Bhat, M., "Output Feedback-Based Discrete-Time Sliding-Mode Controller Design for Model Aircraft," *Journal of Guidance, Control, and Dynamics*, Vol. 28, No. 1, 2005, pp. 177–181.
- [3] Innocenti, M., Pollini, L., and Turra, D., "Guidance of Unmanned Air Vehicles Based on Fuzzy Sets and Fixed Waypoints," *Journal of Guidance, Control, and Dynamics*, Vol. 27, No. 4, 2004, pp. 715–720.
- [4] Ikonen, E., and Najim, K., *Advanced Process Identification and Control*, Marcel Dekker, New York, 2002, pp. 181–197.
- [5] Chen, H., and Allgöwer, F., "Quasi-Infinite Horizon Nonlinear Model Predictive Control Scheme with Guaranteed Stability," *Automatica: the Journal of IFAC, the International Federation of Automatic Control*, Vol. 34, No. 10, 1998, pp. 1205–1217.
- [6] Cloutier, J. R., "State-Dependent Riccati Equation Techniques: An Overview," *Proceedings of the American Controls Conference*, Vol. 2, IEEE, Piscataway, NJ, 1997, pp. 932–936.
- [7] Sznaier, M., Cloutier, J., Hull, R., Jacques, D., and Mracek, M., "A Receding Horizon State Dependent Riccati Equation Approach to Suboptimal Regulation of Nonlinear Systems," *Proceedings of the 37th IEEE Conference on Decision & Control*, Vol. 2, IEEE, Piscataway, NJ, 1998, pp. 1792–1797.
- [8] Kouvaritakis, B., Cannon, M., and Rossiter, J. A., "Non-Linear Model Based Predictive Control," *International Journal of Control*, Vol. 72, No. 10, 1999, pp. 919–928.
- [9] Brooms, A. C., and Kouvaritakis, B., "Successive Constrained Optimization and Interpolation in Non-Linear Model Based Predictive Control," *International Journal of Control*, Vol. 73, No. 4, 2000, pp. 312–316.
- [10] Cannon, M., Kouvaritakis, B., Lee, Y. I., and Brooms, A. C., "Efficient Non-Linear Model Based Predictive Control," *International Journal of Control*, Vol. 74, No. 4, 2001, pp. 361–372.
- [11] Magni, L., De Nicolao, G., Scattolini, R., and Allgöwer, F., "Robust Model Predictive Control for Nonlinear Discrete-Time Systems," *International Journal of Robust and Nonlinear Control*, Vol. 13, Nos. 3–4, March–April 2003, pp. 229–246.
- [12] Xin, M., and Balakrishnan, S. N., "A New Method for Suboptimal Control of a Class of Nonlinear Systems," *Proceedings of IEEE Conference on Decision and Control*, Vol. 3, IEEE Control System Society, IEEE, Piscataway, NJ, 2002, pp. 2756–2761.
- [13] Patwardhan, A. A., Rawlings, J. B., and Edgar, T. F., "Nonlinear Model Predictive Control," *Chemical Engineering Communications*, Vol. 87, 1990, pp. 123–141.
- [14] Patwardhan, A. A., and Madhavan, K. F., "Nonlinear Model Predictive Control Using Second-Order Model Approximation," *Industrial and Engineering Chemistry Research*, Vol. 32, No. 2, Feb. 1993, pp. 334–344.
- [15] Mutha, R. K., Cluett, W. R., and Penlidis, A., "Nonlinear Model-Based Predictive Control of Control Nonaffine Systems," *Automatica: the Journal of IFAC, the International Federation of Automatic Control*, Vol. 33, No. 5, 1997, pp. 907–913.
- [16] Chen, W. H., "Predictive Control of a General Nonlinear System Using Approximation," *IEE Proceedings-Control Theory and Applications*, Vol. 151, No. 2, March 2004, pp. 233–239.
- [17] Lissaman, P. B. S., and Brown, G. J., "Apparent Mass Effects on Parafoil Dynamics," AIAA Paper 93-1236, 1993.